

Original Article

Evaluation of histone deacetylase inhibitory and antiproliferative activity of piperine and its derivatives

La-or Somsakeesit^{1*}, Anupong Joompang², Santi Phosri³, Pattaravadee Srikoon²,
Pakit Kumboonma⁴, Thanaset Senawong⁵, and Chanokbhorn Phaosiri⁶

¹ Department of Chemistry, Faculty of Engineering,
Rajamangala University of Technology Isan Khon Kaen Campus, Mueang, Khon Kaen, 40000 Thailand

² Faculty of Pharmaceutical Sciences, Burapha University, Mueang, Chonburi, 20131 Thailand

³ Department of Chemical Engineering, Faculty of Engineering,
Burapha University, Mueang, Chonburi, 20131 Thailand

⁴ Department of Applied Chemistry, Faculty of Science and Liberal Arts,
Rajamangala University of Technology Isan, Mueang, Nakhon Ratchasima, 30000 Thailand

⁵ Natural Products Research Unit, Department of Biochemistry, Faculty of Science,
Khon Kaen University, Mueang, Khon Kaen, 40002 Thailand

⁶ Natural Products Research Unit, Department of Chemistry, Faculty of Science,
Khon Kaen University, Mueang, Khon Kaen, 40002 Thailand

Received: 2 July 2022; Revised: 22 October 2022; Accepted: 1 November 2022

Abstract

Piperine (**1**) was obtained from the seeds of *Piper nigrum* L. It could act as a pan-histone deacetylase (HDAC) inhibitor. This lead compound was structurally modified to six derivatives that exhibited improved HDAC inhibitory activity. Based on the preliminary results, amide derivatives (**1e** and **1f**) with the highest HDAC inhibitory activity were further studied. The results indicated that the derivatives **1e** and **1f** showed HDAC inhibitory activity with IC₅₀ of 85.61 ± 3.32 μM and 111.27 ± 2.13 μM, respectively. A molecular docking study suggested that piperine (**1**) had a high selectivity for HDAC1, while **1e** and **1f** showed high selectivity for HDAC2. These derivatives were predicted to interact with HDAC active site using hydrogen bond, hydrophobic interaction, as well as chelation with Zn²⁺. The antiproliferative activity obtained from MTT assay against the HeLa cell line indicated that **1f** potentially inhibits HeLa cells with an IC₅₀ of 10.38 ± 2.13 μg/mL. These results suggest potential HDAC inhibitors for further development to anti-cancer agents.

Keywords: *piper nigrum* l., piperine, piperine derivative, HDAC, hela cell

*Corresponding author

Email address: laor.so@rmuti.ac.th

1. Introduction

Cancer is the leading cause of death worldwide. In many less developed countries, more women are killed by cervical cancer than by breast, lung, and ovarian cancers combined (Abu-Rustum *et al.*, 2020). Cervical cancer can be divided into two types: squamous cervical cancer and adenocarcinoma. More than 90% of cervical cancers are of the squamous type. Human papillomavirus (HPV) is the primary cause of the development of cervical cancer. The virus is acquired directly through sexual activity (Jalil *et al.*, 2021; Schiffman, Castle, Jeronimo, Rodriguez, & Wacholder, 2007). Epigenetics plays a crucial role in carcinogenesis. The changes of gene expression without altering the DNA sequence are referred to as epigenetics. Deacetylation of the histone protein is one type of epigenetic modifications (Mai *et al.*, 2005). Histone deacetylases (HDACs) are enzymes that play a key role in deacetylation. Eighteen HDAC isoforms have been grouped into four classes based on sequence similarity to the yeast original enzymes and domain structures. Class I (HDAC1, 2, 3, and 8), class IIa (HDAC4, 5, 7, and 9), class IIb (HDAC6 and 10) and class IV (HDAC11) are Zn²⁺-dependent enzymes, while Class III (SIRT 1-7) are nicotinamide adenine dinucleotide (NAD⁺) dependent enzymes (Bondarev *et al.*, 2021; Zhao *et al.*, 2020). HDACs deacetylate histone by removing the acetyl group from lysine residues. This deacetylation provides a positive charge on the lysine of histone, which enhances the strength of interactions between histone and DNA, resulting in compacted chromatin and obstruction of gene transcription (Hai, He, Shu, & Yin, 2021). The overexpression of HDAC is often observed in cancers that are caused by HPV oncoprotein activity (especially E6 and E7), including cervical cancer. The deacetylation of histone protein tails by HDAC can cause inhibition of the transcription of tumor suppressor genes, resulting in tumors evolving into cancer. Therefore, the inhibition of HDAC is targeted for cervical cancer therapy as well as for treating other forms of cancer (Lourenço de Freitas *et al.*, 2021; Zhang *et al.*, 2021).

Currently, a variety of compounds has been reported for HDAC inhibition. Histone deacetylase inhibitors (HDACis) can be divided into four major groups depending on their dissimilar functional groups, consisting of short-chain fatty acids, hydroxamic acids, epoxyketones, and benzamides. Five HDACis have been approved by the FDA, including Vorinostat (SAHA), Belinostat, Chidamide, Romidepsin and Panobinostat (Figure 1) (Omidkhah *et al.*, 2021). These HDACis contain suitable HDAC-inhibitor pharmacophores including a capping group (CAP) to interact with amino in the active site of enzyme, a linker chain to fill out the narrow tunnel, and a zinc-binding group (ZBG) to bind with Zn²⁺ ion in a pocket of the HDAC active site (Zhang *et al.*, 2020, 2021). Although such HDACis have been used in clinical treatment, their toxicity, non-specificity, and side effects have also been reported (Maccallini *et al.*, 2022). Thus, the identification and development of new HDACis is still needed. Most HDACis, such as SAHA and the natural product trichostatin A (TSA), are hydroxamic acid derivatives. Severe toxicity is found to be associated with the hydroxamic acid group. Therefore, natural product compounds derived from vegetables and fruits with non-hydroxamic acid such as kaempferol, curcumin, and hydroxycapsaicin have been

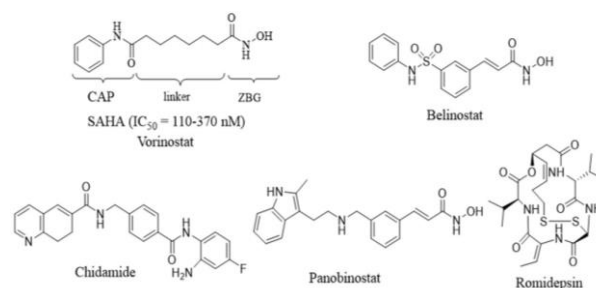


Figure 1. The pharmacophore features of SAHA and the HDAC inhibitors

studied for HDAC inhibitory activity (Berger *et al.*, 2013; Kumboonma, Senawong, Saenglee, & Phaosiri, 2021; Somsakeesit *et al.*, 2020).

Spices are natural food additives that enhance the aroma and flavor of foods. Certain spices have also medicinal and nutritional properties. *Piper nigrum* L., (Piperaceae), commonly called black pepper, has been used as a food additive as well as in traditional medicines to treat fever, cold colic disorder, and gastric conditions (Ashokkumar, Murugan, Dhanya, Pandian, & Warkentin, 2021). Piperine (**1**) is a major alkaloid from black pepper and a natural compound in the non-hydroxamic acid group. It has a wide range of biological activities such as anti-inflammatory, anti-malarial, antimicrobial, and anticancer activity (Turrini, Sestili, & Fimognari, 2020). It has also been used as an agent for the treatment of stomach-ache and weight loss control, and for fever reduction. Interestingly, piperine (**1**), and its analogue have been reported to exhibit anticancer activity (Haq *et al.*, 2021) potentially inhibiting HDAC3/HDAC8 activity (Xiaohui *et al.*, 2018).

According to the knowledge above and based on the various biological activities as well as potent HDAC inhibition, piperine (**1**) is considered an interesting natural lead compound for modification to improve its HDAC inhibitory activity. Therefore, this work focused on the modification of piperine (**1**) from the seeds of black pepper. Such modification is aimed at exploring piperine derivatives with potent histone deacetylase inhibitory activity along with potent anti-proliferative activity against the HeLa cell line.

2. Materials and Methods

2.1 General

All the reagents were purchased from commercial sources (Sigma-Aldrich, Merck, CIL, Carlo Erba and TCI) and used without further purification. Analytical thin layer chromatography (TLC) was conducted on precoated TLC plate using silica gel 60F-254 (E. Merck, Darmstadt Germany). Silica gel column chromatography was carried out on silica gel 60 (230-400 Mesh ASTM, Merck, Germany). The IR spectra were obtained on Perkin Elmer Spectrum Two FT-IR spectrophotometer (USA). NMR spectra were recorded on an NMR spectrometer (Bruker AM400, Switzerland) operated at 400 MHz (¹H) or 100 MHz (¹³C) with TMS solvent at 25 °C. The fluorescence was measured using microplate spectrofluorometer (SpectraMax M5 plate reader, Molecular Devices, USA). Mass spectra were determined

using a Micromass Q-TOF 2 hybrid quadrupole time-of-flight (Q-TOF) mass spectrometer with a Z-spray ES source.

2.2 Plant material

The seeds of *P. nigrum* L. were bought from a local market in Khon Kaen Province, Thailand. Piperine (**1**) was extracted from the dried powder of *P. Nigrum* L. seeds (1.00 kg) using glacial acetic acid followed by purification using diethyl ether recrystallization to obtain piperine (**1**, 18.50 g, yield: 4 %). Its structure was identified using spectroscopy techniques and compared with a previous report (Paarakh, Sreeram, & Ganapathy, 2015).

2.3 Structural modifications

Compounds **1a-1f** were prepared by hydrolysis, esterification and amidation, as shown in Figure 2. All the compounds were characterized by using the spectroscopy techniques IR, NMR, and MS.

2.3.1 General procedure for the synthesis of piperic acid (**1a**)

The solution of piperine (**1**) (1.02 g, 3.96 mmol) was dissolved in methanol and then potassium hydroxide (0.22 g, 3.96 mmol) was added. The reaction was refluxed until the it was completed based on TLC detection. The reaction product was concentrated under vacuum and then quenched with 10 mL of water. After the aqueous solution was acidified with 5% hydrochloric acid (v/v), the pale-yellow solid was obtained by filtration, washed with distilled water, and dried in a vacuum to provide piperic acid (**1a**, 0.79 g, 92 % yield). Its structure was compared with previous reports (Qin, Yang, & Cao, 2020).

2.3.2 General procedure for the synthesis of **1b-1d**

As shown in Figure 2, to the solution of piperic acid (**1a**, 102 mg, 0.47 mmol) in methanol, sulfuric acid was added. The blend was refluxed until the reaction was completed based on TLC detection. Subsequently, the reaction product was concentrated under vacuum and quenched with distilled water. After that the aqueous solution was extracted with dichloromethane (3 x 10 mL) and the combined organic layers were washed with 5% sodium hydrogen carbonate (10 mL). The organic layers were further dried using anhydrous sodium sulfate and concentrated. Purification of the crude product was performed using column chromatography (10% ethyl acetate/hexane as eluent) to obtain compound **1b** (120 mg, yield 81%). Derivatives **1c** (105 mg, yield 93 %) and **1d** (101 mg, yield 91 %) were prepared similar to **1b** using ethanol and butanol instead of methanol in the reaction with piperic acid (**1a**) (Sivashanmugam & Velmathi, 2021).

2.3.3 General procedure for the synthesis of **1e-1f**

As shown in Figure 2, the piperic acid (**1a**, 245 mg, 1.12 mmol) was dissolved in 5 mL of dichloromethane, and then *N,N'*-dicyclohexylcarbodiimide (1.35 mmol) and 4-dimethylaminopyridine (1.35 mmol) were added into the

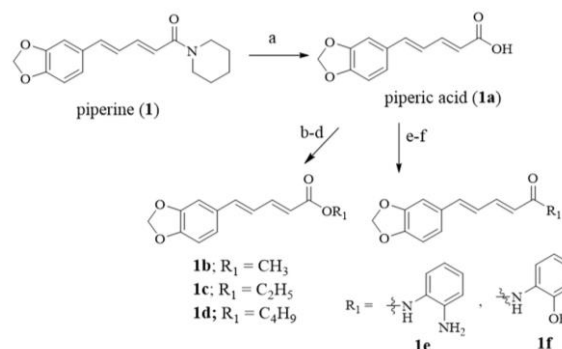


Figure 2. Reagents and conditions: (a) CH₃OH, KOH, reflux, 24 h, 92 %; (b) CH₃OH, H₂SO₄, reflux, 2 h, 81 %; (c) C₂H₅OH, H₂SO₄, reflux, 2 h, 93 %; (d) C₄H₉OH, H₂SO₄, reflux, 2 h, 91 %; (e) *o*-phenylenediamine, DCC, DMAP, DCM, RT, 6 h, 25 %; (f) 2-aminophenol, DCC, DMAP, DCM, RT, 6 h, 27 %

reaction. After 5 minutes, *o*-phenylenediamine was added into the reaction. This mix was stirred until the reaction was completed based on TLC detection. After that the solution was filtered and quenched by adding distilled water (10 mL). The solution was extracted with dichloromethane (10 mL x 2). Next, the organic layer was washed with 5% sodium hydrogen carbonate (10 mL) and 5% hydrochloric acid (10 mL) and then dried using anhydrous sodium sulfate. The filtrate was concentrated under reduced pressure and purified by column chromatography using silica gel with ethyl acetate and hexane (3:7) as an eluent to obtain compound **1e** (82 mg, yield 25%) as a brown solid. Furthermore, compound **1f** (84 mg, yield: 27 %) was prepared in parallel with **1e** by utilizing 2-aminophenol in the reaction of piperic acid (**1a**) (Qin *et al.*, 2020).

(2*E*,4*E*)-*N*-(2-aminophenyl)-5-(benzo[d][1,3]dioxol-5-yl)penta-2,4-dienamide (**1e**)

*R*_f 0.35 (3:7 (v/v) ethyl acetate/hexane. IR (neat) 3405, 2931, 2855, 1652, 1453, 1252 cm⁻¹. ¹H NMR (400 MHz, DMSO-*d*₆) δ 9.34 (s, 1H), 7.31-7.27 (m, 2H), 7.03-6.99 (m, 2H), 6.96-6.86 (m, 4H), 6.74 (dd, *J* = 8.0, 1.2 Hz, 1H), 6.57 (td, *J* = 7.7, 1.4 Hz, 1H), 6.35 (d, *J* = 14.9 Hz, 1H), 6.05 (s, 2H), 4.92 (s, 2H). ¹³C NMR (100 MHz, DMSO-*d*₆) δ 163.6 (C₁), 147.8 (C_{3a}), 147.7 (C_{7a}), 141.5 (C_{2'}), 140.4 (C₃), 138.4 (C₅), 130.7 (C_{5'}), 125.6 (C_{6'}), 125.0 (C_{4'}), 124.6 (C₄), 124.2 (C_{6'}), 123.4 (C_{1''}), 122.7 (C₂), 116.1 (C_{5''}), 115.9 (C_{3''}), 108.3 (C₇), 105.5 (C_{4'}), 101.1 (C_{2'}); HRMS-ESI (*m/z*) [M+H⁺] calcd for C₁₈H₁₇N₂O₃ 309.1239, found 309.1237.

2.4 Histone deacetylase activity assay

Piperine (**1**) and all derivatives (**1a-1f**) were evaluated for their HDAC inhibitory activity using a Fluor-de-Lys HDAC activity assay kit (Biomol, Enzo Life Science International, Inc., USA). Pan-HDAC enzymes were obtained from HeLa nuclear extract. Briefly, all derivatives were evaluated using 100 μM as the final concentration for screening. Trichostatin A (TSA) was used as a positive control at 0.125 μM. Five microliters of Piperine (**1**) and its derivatives (inhibitors), 1 μL of the HeLa nuclear extract and 19 μL of buffer were added to a 96-well plate and incubated at

37 °C for 5 minutes. After incubation, 25 µL of the substrate was added and incubated at 37 °C for 15 minutes. Then, 50 µL of the developer was added for fluorophore generation. Finally, the reaction was detected for the fluorescence signal using a fluorescence spectrometer. The fluorescence signal was measured with excitation at 360 nm and emission at 460 nm (Somsakeesit *et al.*, 2020).

2.5 Molecular docking studies

All 2D structures of compounds were built using the ChemDraw program (ChemDraw professional 17.1), and were transferred into Hyperchem 8.0 software (HyperChem, Release 8.0 for Windows, Molecular Modeling System: HyperCube, 2007) using optimized energy (Asadzadeh *et al.*, 2015). The Auto Dock Tools 1.5.6 (ADT) and Auto Dock 4.2 programs were used for molecular docking for 50 runs. The size of the grid box was set at 60 x 60 x 60 points and a Lamarckian genetic algorithm search was used. The crystal structures of human histone deacetylase HDAC1 [PDB entry code: 4bkx], HDAC2 [PDB entry code: 3max complexed with the inhibitor, LLX400], HDAC3 [PDB entry code: 4a69 complexed with the inhibitor, 10P501], and HDAC8 [PDB entry code: 1t69 complexed with the inhibitor, SAHA, resolution: 2.91 Å] were obtained from the Protein Data Bank. All water and non-interacting ions as well as TSA were removed. Afterward, all missing hydrogen and side chain atoms were added using the ADT program. Gasteiger charges were calculated for the system. Compound–HDAC interaction was detected using Discovery Studio 2017 R2 Client (Somsakeesit *et al.*, 2020).

2.6 Cell culture

HeLa cells and Vero cells were purchased from the American Type Culture Collection (ATCC, Manassas, VA, USA). These cells were cultured in RPMI 1640 supplemented with 10% heat-inactivated FBS, 1% penicillin-streptomycin under 37 °C, 5% CO₂ and 90% relative humidity.

2.7 Antiproliferative activity using MTT assay

The antiproliferative activity of piperine (**1**), **1e**, and **1f** was tested against the human cervical cancer (HeLa) cell line. Briefly, cells were seeded into 96-well plates overnight. Then, the cells were treated with different concentrations (0–100 µg/mL) of the compound and incubated for 24, 48, and 72 h. After incubation, the medium was removed and MTT solution (0.5 mg/mL) was added and incubated for 2 h. After 2 h, DMSO was added and the absorbance at 550 with a reference wavelength at 655 nm was recorded. Relative cell viability was calculated and compared with untreated cells. The IC₅₀ for each treatment group was calculated.

The toxicity of piperine (**1**), **1e**, and **1f** was tested against Vero cells. The Vero cells were seeded into 96-well plates overnight. Subsequently, the experiment was performed similarly to the antiproliferative activity against HeLa cells. Relative cell viability was calculated and compared with the untreated cells (Phaosiri *et al.*, 2022).

3. Results and Discussion

3.1 Chemistry

Piperine (**1**) was obtained from the seeds of *P. nigrum* L. Synthesis of piperine derivatives was done as shown in Figure 2. A mixture of piperine (**1**) in methanol and potassium hydroxide produced piperic acid (**1a**). Compound **1a** was reacted with methanol, ethanol, and butanol under acidic conditions to produce ester derivatives (**1b-1d**). According to ¹H NMR of **1b-1d**, it was found that acetal remained intact, as the observed chemical shift was at δ 5.98 (s, 2H_{2'}) ppm for compound **1b**, and at δ 5.97 (s, 2H_{2'}) ppm for compounds **1c** and **1d**. The results indicate that acidic condition cannot hydrolyze the acetal group.

Compound **1a** was reacted with *o*-phenylenediamine and 2-aminophenol using coupling reagents to produce amide derivatives (**1e-1f**). Spectroscopic techniques were used to identify all compounds and were compared to previous reports for compounds **1a-1d** and **1f** (Qin *et al.*, 2020; Sivashanmugam, & Velmathi, 2021). The newly synthesized **1e** was fully identified with IR, NMR, and MS techniques.

3.2 HDAC inhibitory activity

According to the docking of TSA with HDAC2 it was found that the TSA hydroxamic group was located around the Zn²⁺ binding site and its hydroxyl group was located near to Zn²⁺, suggesting chelation between hydroxyl and Zn²⁺. In the crystal structure of TSA and HDAC2 (PDB: 3max), Zn²⁺ was chelated by the hydroxyl of the hydroxamic group. Chelation occurred along with hydrogen around the Zn²⁺ binding site. When considering piperine (**1**) with HDAC1, the results showed that the piperidine ring was located near Zn²⁺ with hydrophobic interaction and Zn²⁺ was observed to interact with its carbonyl of amide via chelation. No hydrogen bond was found along with the interaction with Zn²⁺. Piperine (**1**) showed much less HDAC inhibitory activity than TSA. Therefore, we expected that the interaction with Zn²⁺ along with the hydrogen bond around the Zn²⁺ binding site might provide stronger HDAC inhibitory activity. As a result, the piperidine moiety of piperine (**1**) was modified into the methyl, ethyl, butyl esters and 2-aminophenyl, 2-hydroxyphenyl amides (Table 1) in order to obtain a hydrogen bond, while maintaining hydrophobic interaction and the interaction with Zn²⁺. Methyl, ethyl, and butyl esters showed more flexibility than the piperidine ring. This increased flexibility might facilitate hydrogen bond formation, while their side chains provide hydrophobic interaction. According to the literature review, HDAC inhibitors with benzamides showed strong inhibition with less toxicity (Zhang *et al.*, 2019). Therefore, 2-aminophenyl, 2-hydroxyphenyl amides were used for the modification. These modifications were expected to achieve hydrogen bond formation from the hydroxyl and amino groups, while hydrophobic interactions and Pi-Pi interaction were obtained from the phenyl ring.

The modification resulted in six derivatives as shown in Figure 2. Piperine (**1**) and its derivatives (**1a-1f**) at 100 µM were screened for inhibition against HDACs from

Table 1. Histone deacetylase inhibitory activity of piperine (1) and its derivatives

Compound	R ₁	% HDAC inhibition
Piperine (1)	-	14.47 ± 0.08
1a	-	39.72 ± 0.44
1b	CH ₃	48.73 ± 0.35
1c	C ₂ H ₅	42.62 ± 0.53
1d	C ₄ H ₉	39.67 ± 0.38
1e		79.21 ± 0.22
1f		72.85 ± 0.10

HeLa nuclear extract. The results indicated that all derivatives (**1a-1f**) showed HDAC inhibitory activity higher than piperine (**1**). The positive control, TSA, at 0.125 μM showed strong inhibition by 86 ± 0.06%. According to the modification, amide derivatives (**1e-1f**) provided the highest inhibitory activity (Table 1). Therefore, derivatives **1e** and **1f** were further evaluated for their IC₅₀ values. It was found that derivatives **1e** and **1f** showed IC₅₀ values of 85.61 ± 3.32 μM and 111.27 ± 2.13 μM, respectively, being more potent than piperine (**1**) (IC₅₀ of 352.80 ± 4.33 μM) (Table 2). According to previous reports, SAHA, TSA, Kaemperol, curcumin, and hydroxycapsaicin showed HDAC IC₅₀ ranging from nanomolar to millimolar level (Berger *et al.*, 2013; Kumboonma *et al.*, 2021; Somsakeesit *et al.*, 2020). Compounds **1e** and **1f** showed HDAC inhibitory activity with IC₅₀ in micromolar level (Table 2). Therefore, compounds **1e** and **1f** are considered interesting compounds compared to various natural compounds, although they exhibited less inhibitory activity than SAHA and TSA. These results suggest that the modification successfully increased the HDAC inhibitory activity and that **1e** and **1f** are the interesting HDAC inhibitors.

3.3 Molecular docking

The molecular docking results are shown in Table 2 and Figure 3. The results suggest that piperine (**1**) had the lowest binding energy of -9.48 kcal/mol and K_i of 0.11 μM with HDAC1. Compound **1e** had the lowest binding energy of

-9.36 kcal/mol and K_i of 0.14 μM with HDAC2, while **1f** had the lowest binding energy of -9.83 kcal/mol and K_i of 0.06 μM with HDAC2. A molecular docking experiment predicted that piperine (**1**) and its derivatives **1e** and **1f** mainly interacted with the enzyme-active site using hydrogen bond and hydrophobic interaction (Figure 3A, 3B, and 3C).

According to molecular docking stimulation, it is suggested that all compounds used carbonyl oxygen interaction with Zn²⁺. The amino group of *o*-phenylenediamine and carbonyl of amides **1e** and **1f** were nearly located with Zn²⁺, suggesting the possible chelation of **1** and **1f** with Zn²⁺. Chelation between the hydroxyl of inhibitor with Zn²⁺ was found in SAHA (Lauffer *et al.*, 2013). Although the piperine (**1**) was predicted to bind with the HDAC1 active site using a similar direction with **1e** and **1f** to bind with HDAC2 active, the types and numbers of interactions were different, even though their active sites shared high sequence identity (94%). Amino acid sequence determined protein conformation. Therefore, the difference in types and numbers of interactions between the piperine (**1**) and **1e** and **1f** might be caused by different protein folding, resulting from the slight difference in their amino acid sequences. Moreover, it might also be caused by different functional groups, which were used to modify piperine (**1**) at amide position. This also rendered some different interactions between **1e** and **1f**, even though these compounds interacted in a similar manner with HDAC2.

Regarding molecular docking of the known inhibitor TSA of HDAC2, the results suggested that TSA bound with the HDAC2 active site using hydrophobic interaction and hydrogen bond. Its hydroxyl group was located near Zn²⁺ (Figure 3D). This hydroxyl oxygen chelated with Zn²⁺, as observed in the crystal structure of TSA and HDAC2 (PDB: 3max). Chelation occurred along with the hydroxyl group around the Zn²⁺ binding site. The modification of piperine provided **1e** and **1f**, which showed greater HDAC inhibition than piperine (**1**). Compounds **1e** and **1f** were predicted to interact with Zn²⁺ along with hydrogen bonds around the Zn²⁺ binding site similar to TSA. This hydrogen bond was not observed in piperine (**1**). Therefore, the interaction with Zn²⁺ along with hydrogen bonds around the Zn²⁺ binding site might be one of the key interactions in the strong inhibition to bind and inhibit HDACs. Molecular docking results provided interaction information between HDACs and piperine (**1**), **1e**, and **1f**, which might be beneficial for designing stronger HDAC inhibitors.

Table 2. *In silico* histone deacetylase inhibitory activity of the selected compounds

Cpd	IC ₅₀ **	Class I HDACs							
		HDAC1		HDAC2		HDAC3		HDAC8	
		ΔG*	K _i **	ΔG*	K _i **	ΔG*	K _i **	ΔG*	K _i **
TSA****	-	-8.12	1.12	-8.75	0.39	-8.23	0.93	-8.85	0.33
1	352.80 ± 4.33	-9.48	0.11	-9.41	0.13	-6.97	7.79	-8.83	0.33
1e	85.61 ± 3.32	-8.74	0.39	-9.36	0.14	-7.12	6.08	-8.45	0.64
1f	111.27 ± 2.13	-9.25	0.16	-9.83	0.06	-7.42	3.61	-9.72	0.07

*(kcal/mol), ** (μM), *** (from Phaosiri *et al.*; 2022)

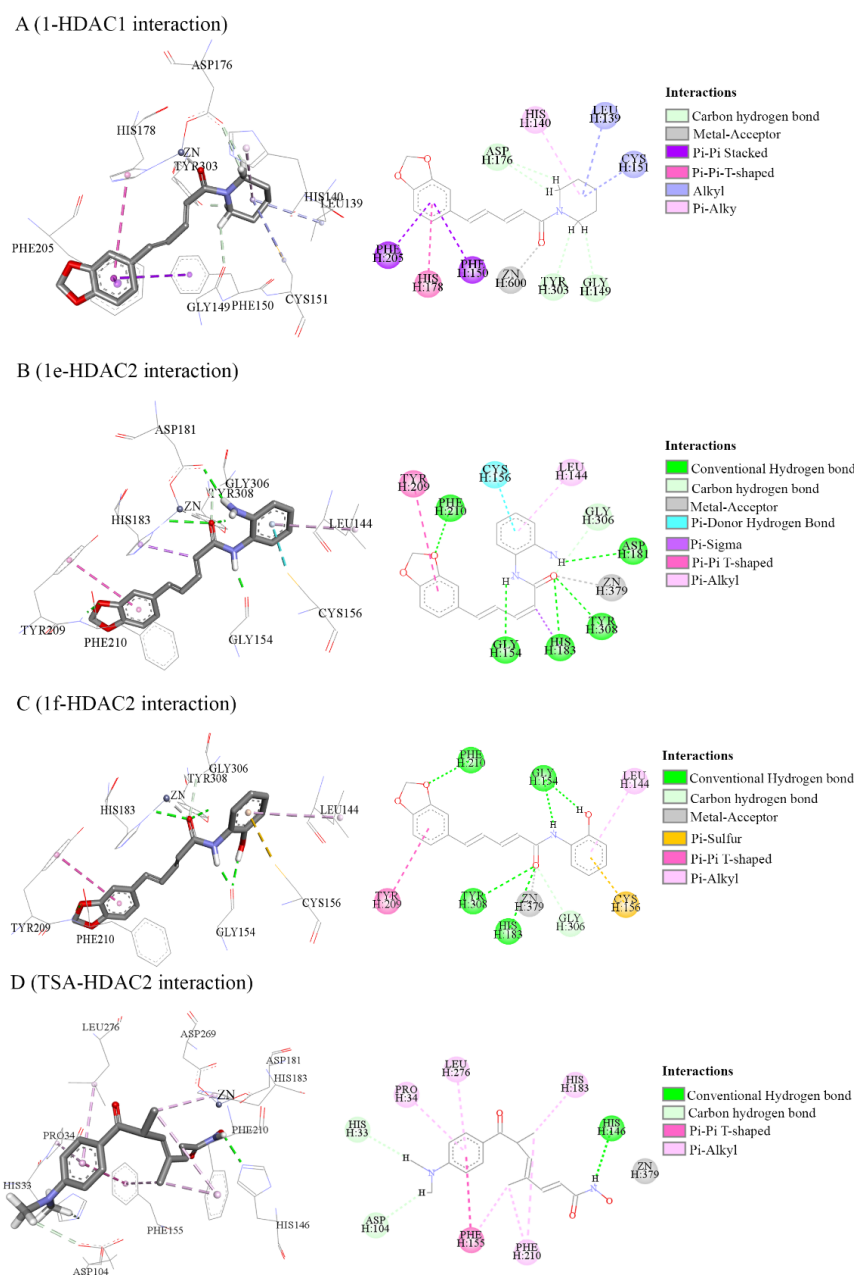


Figure 3. Piperine (**1**), **1e**, and **1f** HDAC interactions. (A) 1-HDAC1, (B) 1e-HDAC2, (C) 1f-HDAC2, and (D) TSA-HDAC2 interaction. The figure was made using Discovery Studio 2017 R2 Client

3.4 Antiproliferative activity against HeLa cells

Piperine (**1**) and its amide derivatives, **1e** and **1f** were initially evaluated for toxicity against normal cells, using Vero cells as a model. The results show that cell viability decreased with the concentration of piperine (**1**), **1e**, and **1f** along with an increase in incubation time (Figure 4). For compound **1f**, no toxicity was observed after 24 or 48 h of incubation on using concentrations of 20 - 60 $\mu\text{g/mL}$, nor after 72 h of incubation on using concentrations of 20 - 40 $\mu\text{g/mL}$. Comparing toxicity, the highest cytotoxicity was found for piperine (**1**), followed by **1e** and **1f**. Therefore, this suggests

that the amide modification had decreased the cytotoxicity of piperine (**1**) against normal Vero cells. Subsequently, piperine (**1**) and its amide derivatives, **1e** and **1f** were assayed for antiproliferative activity against the HeLa cancer cell line. The results of antiproliferative activity are exhibited in Table 3. For all incubation periods (24, 48, and 72 h), **1f** showed the highest antiproliferative activity, followed by **1e** and piperine (**1**) in rank order. An increase in incubation time increased the antiproliferative activity. These results suggest that the amide modification could enhance antiproliferative activity against HeLa cells. For all incubation times, piperine (**1**) and **1e** were observed to have antiproliferative activity with IC_{50} values in

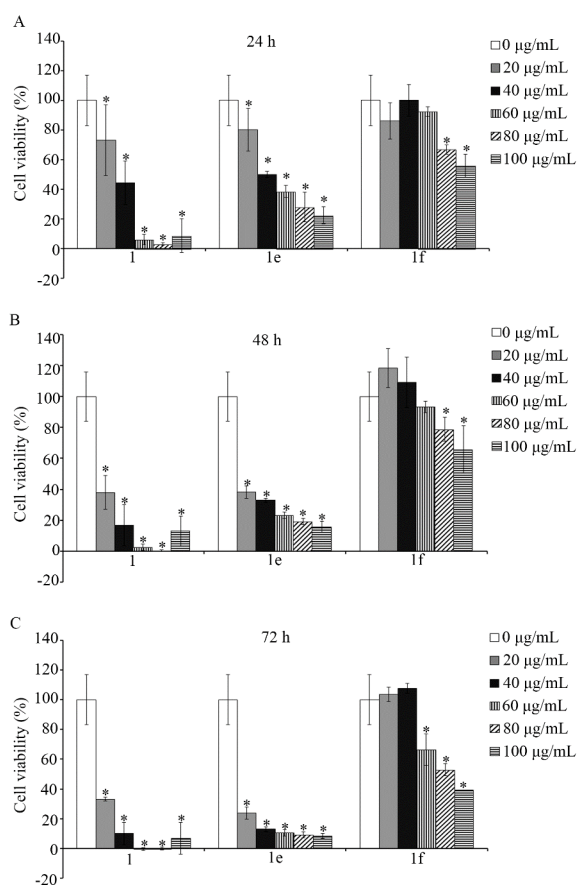


Figure 4. Cell viability of Vero cell. Cells were treated with different concentration of compound (0-100 µg/mL) for 24 h (A), 48 h (B), and 72 h (C). Asterisk (*) indicates a significant difference ($p < 0.05$) according to Duncan's test. The comparison was carried out between control (0 µg/mL) and treatment (20-100 µg/mL) for each compound

Table 3. Antiproliferative activities of piperine (1), 1e, and 1f against Hela cell line

Compound	IC ₅₀ values (mean ± SD; n = 3 (mg/mL))		
	24 h	48 h	72 h
1	35.34 ± 1.12	28.34 ± 1.00	27.84 ± 0.33
1e	64.16 ± 5.79	33.98 ± 0.93	24.14 ± 2.40
1f	31.08 ± 4.48	12.89 ± 0.49	10.38 ± 2.13

the range of toxic concentration toward Vero cells, while the IC₅₀ value of **1f** was found in the range of its non-toxic concentrations. Thus, compound **1f** is an interesting candidate for further development as a cancer treatment agent.

4. Conclusions

Modifications of piperine (**1**) provided carboxylic (**1a**), four ester (**1b** - **1d**) and two amide (**1e** and **1f**) derivatives with improved HDAC inhibitory activity and antiproliferative activities against the HeLa cancer cell line. In addition, compound **1e** was a newly synthesized derivative, with its HDAC inhibitory activity and antiproliferative

activity reported here for the first time. According to HDAC inhibitory activity and antiproliferative activity along with toxicity, compounds **1e** and **1f** are interesting candidates for further development as anti-cancer agents.

Acknowledgements

The authors gratefully acknowledge Rajamangala University of Technology Isan (RMUTI) for its financial support of this work. We would also like to thank Prof. Dr. Somdek Kanokmehakul for providing the piperine standard. Gratitude is also extended to Mr. Kittisak Poopasith for the excellent NMR data and Mr. Sookkawath Walunchapruk for the antiproliferation test. This research project was supported by Rajamangala University of Technology Isan under Contract No. ENG03/64.

References

- Abu-Rustum, N. R., Yashar, C. M., Bean, S., Bradley, K., Campos, S. M., Chon, H. S., . . . Motter, A. D. (2020). NCCN guidelines insights: cervical cancer, version 1.2020: featured updates to the NCCN Guidelines. *Journal of the National Comprehensive Cancer Network*, 18(6), 660-666.
- Asadzadeh, A., Fassihi, A., Yaghmaei, P., & Pourfarzam, M. (2015). Docking studies of some novel kojic acid derivatives as possible tyrosinase inhibitors. *Biomedical and Pharmacology Journal*, 8(2), 535-545. doi:10.13005/bpj/796
- Ashokkumar, K., Murugan, M., Dhanya, M. K., Pandian, A., & Warkentin, T. D. (2021). Phytochemistry and therapeutic potential of black pepper [*Piper nigrum* (L.)] essential oil and piperine: a review. *Clinical Phytoscience*, 7(1), 1-11. doi:10.1186/s40816-021-00292-2
- Berger, A., Venturelli, S., Kallnischkies, M., Böcker, A., Busch, C., Weiland, T., . . . Bitzer, M. (2013). Kaempferol, a new nutrition-derived pan-inhibitor of human histone deacetylases. *The Journal of Nutritional Biochemistry*, 24(6), 977-985. doi:10.1016/j.jnutbio.2012.07.001
- Bondarev, A. D., Attwood, M. M., Jonsson, J., Chubarev, V. N., Tarasov, V. V., & Schiöth, H. B. (2021). Recent developments of HDAC inhibitors: Emerging indications and novel molecules. *British Journal of Clinical Pharmacology*, 87(12), 4577-4597. doi:10.1111/bcp.14889
- Hai, R., He, L., Shu, G., & Yin, G. (2021). Characterization of histone deacetylase mechanisms in cancer development. *Frontiers in Oncology*, 2839. doi:10.3389/fonc.2021.700947
- Haq, I. U., Imran, M., Nadeem, M., Tufail, T., Gondal, T. A., & Mubarak, M. S. (2021). Piperine: A review of its biological effects. *Phytotherapy Research*, 35(2), 680-700. doi:10.1002/ptr.6855
- Jalil, A. T., Kadhun, W. R., Faryad Khan, M. U., Karevskiy, A., Hanan, Z. K., Suksatan, W., . . . Abdullah, M. M. (2021). Cancer stages and demographical study of HPV16 in gene L2 isolated from cervical cancer in Dhi-Qar province, Iraq. *Applied Nanoscience*, 1-7. doi:10.1007/s13204-021-01947-9

- Kumboonma, P., Senawong, T., Saenglee, S., & Phaosiri, C. (2021). Discovery of new capsaicin and dihydrocapsaicin derivatives as histone deacetylase inhibitors and molecular docking studies. *Organic Communications*, 14(2), 143. doi:10.25135/acg.oc.102.21.031998
- Lauffer, B. E., Mintzer, R., Fong, R., Mukund, S., Tam, C., Zilberleyb, I., . . . Steiner, P. (2013). Histone deacetylase (HDAC) inhibitor kinetic rate constants correlate with cellular histone acetylation but not transcription and cell viability. *Journal of Biological Chemistry*, 288(37), 26926-26943. doi:10.1074/jbc.M113.490706
- Lourenço de Freitas, N., Deberaldini, M. G., Gomes, D., Pavan, A. R., Sousa, Â., Dos Santos, J. L., & Soares, C. P. (2021). Histone deacetylase inhibitors as therapeutic interventions on cervical cancer induced by human papillomavirus. *Frontiers in Cell and Developmental Biology*, 8, 592868. doi:10.3389/fcell.2020.592868
- Maccallini, C., Ammazalorso, A., De Filippis, B., Fantacuzzi, M., Giampietro, L., & Amoroso, R. (2022). HDAC Inhibitors for the Therapy of Triple Negative Breast Cancer. *Pharmaceuticals*, 15(6), 667. doi:10.3390/ph15060667
- Mai, A., Massa, S., Rotili, D., Cerbara, I., Valente, S., Pezzi, R., . . . Ragno, R. (2005). Histone deacetylation in epigenetics: an attractive target for anticancer therapy. *Medicinal Research Reviews*, 25(3), 261-309. doi:10.1002/med.20024
- Omidkhah, N., Hadizadeh, F., & Ghodsi, R. (2021). Dual HDAC/BRD4 inhibitors against cancer. *Medicinal Chemistry Research*, 30(10), 1822-1836. doi:10.1007/s00044-021-02776-9
- Paarakh, P. M., Sreeram, D. C., & Ganapathy, S. P. (2015). In vitro cytotoxic and in silico activity of piperine isolated from Piper nigrum fruits Linn. *In Silico Pharmacology*, 3(1), 1-7. doi:10.1186/s40203-015-0013-2
- Phaosiri, C., Yenjai, C., Senawong, T., Senawong, G., Saenglee, S., Somsakeesit, L. O., & Kumboonma, P. (2022). Histone deacetylase inhibitory activity and antiproliferative potential of new [6]-shogaol derivatives. *Molecules*, 27(10), 3332. doi:10.3390/molecules27103332
- Qin, B., Yang, K., & Cao, R. (2020). Synthesis and antioxidative activity of piperine derivatives containing phenolic hydroxyl. *Journal of Chemistry*, 2020. doi:10.1155/2020/2786359
- Schiffman, M., Castle, P. E., Jeronimo, J., Rodriguez, A. C., & Wacholder, S. (2007). Human papillomavirus and cervical cancer. *The Lancet*, 370(9590), 890-907. doi:10.1016/S0140-6736(07)61426-0
- Sivashanmugam, A., & Velmathi, S. (2021). Synthesis, in vitro and in silico anti-bacterial analysis of piperine and piperic ester analogues. *Chemical Biology and Drug Design*, 98(1), 19-29. doi:10.1111/cbdd.13842
- Somsakeesit, L. O., Senawong, T., Kumboonma, P., Saenglee, S., Samankul, A., Senawong, G., . . . Phaosiri, C. (2020). Influence of side-chain changes on histone deacetylase inhibitory and cytotoxicity activities of curcuminoid derivatives. *Bioorganic and Medicinal Chemistry Letters*, 30(11), 127171. doi:10.1016/j.bmcl.2020.127171
- Turrini, E., Sestili, P., & Fimognari, C. (2020). Overview of the anticancer potential of the "king of spices" piper nigrum and its main constituent piperine. *Toxins*, 12(12), 747. doi:10.3390/toxins12120747
- Xiao-hui, Y. A. O., Huan, L. I., Yang-liang, H. U., Ying-jie, H. U., Lin-chun, F. U., & Xiao-ling, S. H. E. N. (2018). Screening of class I HDAC inhibitors from traditional chinese medicine. *Natural Product Research and Development*, 30(7), 1099. doi:10.16333/j.1001-6880.2018.7.001
- Zhang, L., Li, X., Chen, Y., Wan, M., Jiang, Q., Zhang, L., . . . Zhang, L. (2019). Discovery of N-(2-Aminophenyl)-4-(bis (2-chloroethyl) amino) benzamide as a potent histone deacetylase inhibitor. *Frontiers in Pharmacology*, 10, 957. doi:10.3389/fphar.2019.00957
- Zhang, X. H., Qin-Ma, Wu, H. P., Khamis, M. Y., Li, Y. H., Ma, L. Y., & Liu, H. M. (2021). A review of progress in histone deacetylase 6 inhibitors research: structural specificity and functional diversity. *Journal of medicinal chemistry*, 64(3), 1362-1391. doi:10.1021/acs.jmedchem.0c01782
- Zhao, N., Yang, F., Han, L., Qu, Y., Ge, D., & Zhang, H. (2020). Development of coumarin-based hydroxamates as histone deacetylase inhibitors with antitumor activities. *Molecules*, 25(3), 717. doi:10.3390/molecules25030717